27/28th International Conference
ENGINEERING MECHANICS 2022
Milovy, Czech Republic, May 9 –12, 2022
Paper **#56,** pp. 209–212, doi: 10.21495/51-2-209

OPTIMIZATION OF THE SLAY MECHANISM OF THE WEAVING LOOM DIFA

Koňařík T.*

Abstract: *In this paper the development process of a controlled mechanical system of a slay mechanism of a DIFA weaving machine is presented, which is an air-jet loom for a production of special 3D distance fabrics. In order to increase the machine productivity and quality of the woven fabric, a number of modifications were proposed. Simulations of different slay mechanism configurations were carried out and the effects of the modifications on the dynamical behaviour were analysed, resulting in a new optimised design of the machine slay mechanism.*

Keywords: Weaving loom, Slay computational model, Dynamical behaviour.

1. Introduction

The DIFA weaving machine is a shuttle-less loom for the production of special 3D distance fabrics. The key component of the machine is the slay mechanism (Fig. 1). The batten, performing a swinging motion, is actually forming the fabric. Contrary to a classical weaving, 3D fabrics weaving loom uses a non-standard weaving sequence: it starts and stops several times a minute dependent on the pile yarns density.

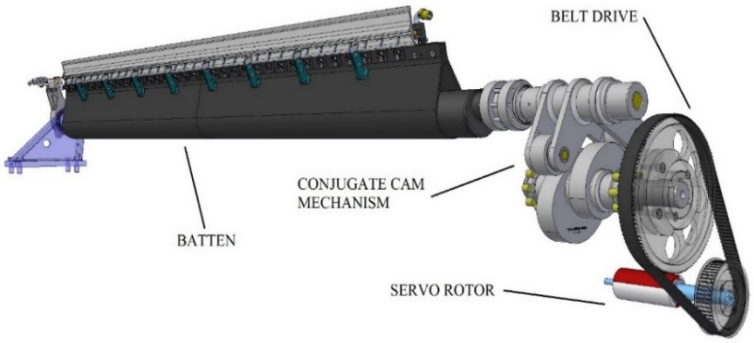

Fig. 1: CAD model of DIFA weaving machine slay mechanism.

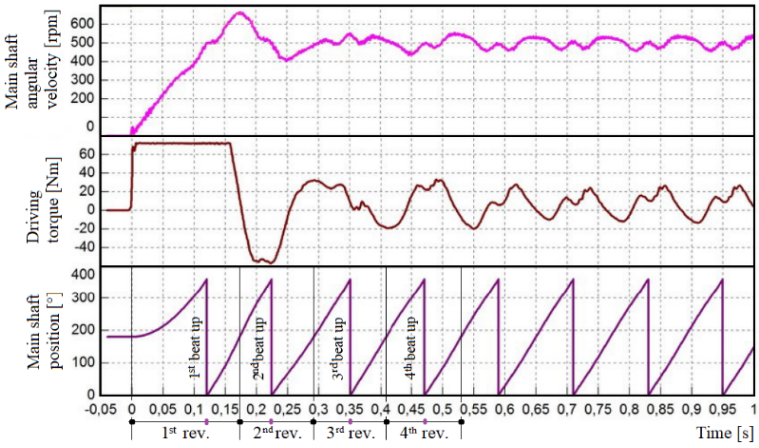

Fig. 2: Measured main shaft angular velocity, drive torque and main shaft position during a start of the machine to nominal 500 rpm (weaving with fabric present).

Current slay mechanisms of the DIFA loom were taken over from the VEGA loom. It was initially designed for high-speed weaving of lighter fabrics. A carbon composite batten with counterbalancing masses is the most dynamically loaded component of the weaving loom and its stiffness is crucial for the final product forming. Part of the slay belt drive is a big belt pulley with additional masses acting like a flywheel. The moment of inertia of that slay mechanism is rather high. Each start and stop generates elevated loads on the cams and bearings so a minimum moment of inertia of the batten and other components of the slay mechanism is at its most desirable. A complex measurement of the dynamical behaviour of the machine has been conducted in order to assess both transition and steady states. That as a base for drawing up improvements to fulfil a demand for increased machine productivity and a quality of the final product as well as for enlarged utility features of 3D fabrics.

* Bc. Tomáš Koňařík, M.Sc.: VÚTS, a.s., Svárovská 619, Liberec, Czech Republic, tomas.konarik@vuts.cz

During each start of the weaving sequence the maximal servomotor drive torque is reached (Fig. 2). Despite the well-tuned starting feed forward control procedure, insufficiently quick first revolution is resulted in the first beat up with less energy, causing negligible quality issue on the woven fabric – noticeably the "starting line". The second issue is that due to a slightly delayed first revolution, the time interval between the first two beat ups becomes shorter, resulting in occasional short picks. Those marginal issues at nominal 500 *rpm* could become significant when the desired weaving speed at nominal 600 *rpm* is reached.

2. Approach

To evaluate the effect of modifications of the slay mechanism on the operation of the DIFA loom, a computational non-linear model of a controlled mechanical system was developed by use of software MSC Adams based on CAD *data* from Siemens Solid Edge and NX. A model of the servo-motor with its control structure was defined by the MSC Easy5 and transferred to the general model using a module MSC Adams/Controls. The slay mechanism is formed by a belt drive mechanism and a cam mechanism with a conjugate cam pair and two roller followers, attached to a common oscillating arm, refer to Fig. 3a. A bigger belt pulley and dual cams are fixed on a common shaft. The cams profile coordinates are determined by kinematic synthesis, which is implemented based on the displacement law $\psi = \psi(\tau)$ knowledge of the slay mechanism and its characteristic dimensional parameters, a =170 *mm*, b =120 *mm*, β =90°, D =80 *mm*. Using the computational model, the effects of the original displacement law:

$$\psi_{Old}(\tau) = 0.2838119 - 0.214737 \cdot \cos(\tau) - 0.069075 \cdot \cos(2\tau), \tag{1}$$

plus the new displacement law:

$$\psi_{New}(\tau) = 0.43633 - \frac{0.43633}{32} \cdot \left[10 + 15 \cdot \cos(\tau) + 6 \cdot \cos(2\tau) + \cos(3\tau)\right] . \tag{2}$$

Based on the dynamic behaviour and properties of the slay mechanism analysis was made, see Fig. 3b. Passive resistances of the mechanism are incorporated in the model, however a weaving resistance is not included.

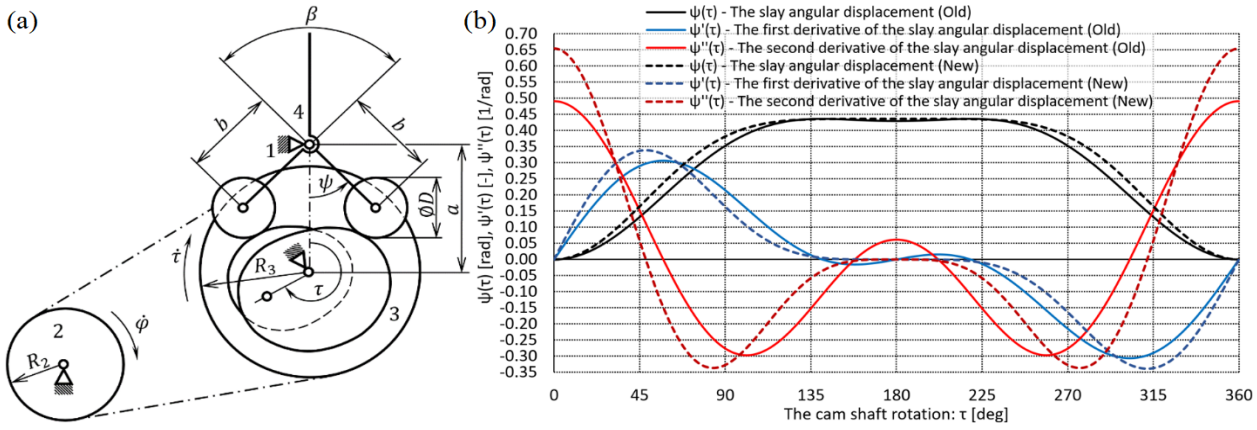

Fig. 2: a) Kinematic diagram of cam mechanism; b) Displacement law (Old – New).

The drive of the slay mechanism is implemented by a 3-phase permanent magnet synchronous electric motor - MSM (TGN5-2400-15-560). Its computational model is defined based on the so-called *dq*-model, which is based on a mathematical description of a synchronous machine and consists in transformation of a 3-phase machine to an equivalent 2-phase machine using complex space phasors (Bose, 2002; Ondrášek and Karel, 2020). Using a 2-phase motor model reduces the number of equations and simplifies the control design. Essentially, variables (current, voltage, flux linkage) associated with the stator windings of a synchronous machine are transformed to a synchronously rotating reference frame (d,q) fixed in the rotor at speed ω_0. During the vector control of this electric motor type in the case of a weaving machine, a cascade control loop is used with three hierarchically arranged feedbacks: current, speed, and position (Ondrášek & Karel, 2020), see Fig. 4. Maintaining the required values of position φ_r^*, revolutions ω^* and current $\mathbf{i}^* = (I_d^*, I_q^*)$ is ensured by PID linear controllers. The control action is thus the sum of the three terms: proportional feedback, the integral term and derivative action. The relation between the output

value $u(t)$ (the control value) and the input value $e(t)$ (the tracking error) is given by the equation (Åström & Murray, 2008):

$$u(t) = K\left(e(t) + \frac{1}{T_i}\int_0^t e(\tau)\mathrm{d}\tau + T_d\frac{\mathrm{d}e(t)}{\mathrm{d}t}\right) + u_f(t), \qquad e(t) = w(t) - y(t)\ . \tag{3}$$

The controller parameters are the proportional gain $r_0 = K$, the integral gain $r_{-1} = K / T_i$ and the derivative gain $r_1 = K \cdot T_d$. The time constants T_i and T_d are called the integral time constant and the derivative time constant. We can tune the appropriate parameters of PID controllers according to the Ziegler–Nichols tuning rules (Åström and Murray, 2008). In Eq. (3), $u_f(t)$ expresses a feed-forward term that is adjusted to give the desired value. The tracking error $e(t)$ expresses the difference between the desired input value ($w(t) = \{\varphi_r^*, \omega^*, \mathbf{i}^*\}$) and the actual output ($y(t) = \{\varphi, \omega, \mathbf{i}\}$) of the controlled system according to Fig. 4. Fig. 4 shows the block diagram of the cascade control loop with ideal P and PI controllers and speed ω_r^* and current $\mathbf{i}_r^*$ feed-forward. The value of the current feed-forward constant k_{Mf} of the control structure is determined based on the electromagnetic moment M_{ElMg} of the 3-phase permanent magnet synchronous electric motor (Ondrášek & Karel, 2020):

$$M_{ElMg} = \frac{3}{2}p_p\Psi_m I_q = \frac{1}{k_{Mf}}I_q, \qquad k_{Mf} = \frac{2}{3p_p\Psi_m}, \qquad \Psi_m = k_E\frac{60}{2\pi 1000\sqrt{3}}, \tag{4}$$

where $k_E = 183\ V1000^{-1}rpm$ expresses the electromotor voltage constant and $p_p = 5$ denotes the number of pole pairs, which are from the data sheet provided by the manufacturer. In Eq. (4), variable Ψ_m is a permanent magnetic flux linkage. The quantities I_d and I_q denote current components expressed in the rotor reference frame (d,q) according to the dq-model of PMSM.

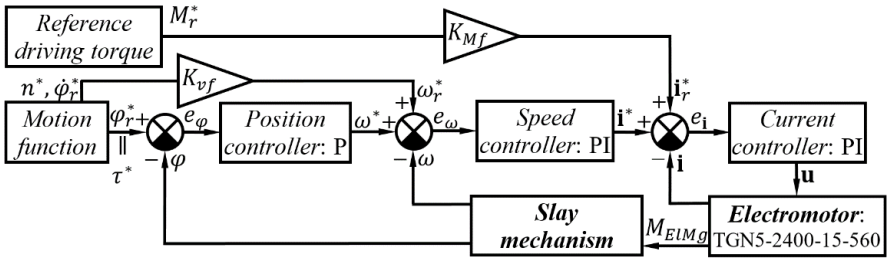

Fig. 3: Slay mechanism drive block diagram.

Simulations were conducted based on different configurations of the mechanical system. In order to achieve the weaving speed at nominal 600 *rpm*, the slay mechanism had to be revised with the major aim to decrease the moment of inertia *I*. Flywheel masses of the big pulley were minimized. The batten was completely redesigned with retained stiffness (Koňařík et al., 2022). Better mass characteristic is achieved when the belt gear ratio is changed to 1:2.5, nevertheless, an electric motor with a higher nominal speed has to be used. In Table 1 there is a list of selected simulation configurations, where the simulation number 00 represents an initial state, 13 and 15 are with all modifications applied, differing in a starting position of the main shaft. Start from 120° gives an additional time for reaching the nominal speed.

Tab. 1: Selected simulation configurations of the slay mechanism.

Simulation number	Mass characteristics of slay mechanism						Displacement law $\psi = \psi(t)$	Belt gear ratio	Main shaft rev. [rpm]	Start		Stop	
	Cam + big pulley		Batten + cam follower		Servo rotor + small pulley					from [deg]	to [deg]	from [deg]	to [deg]
	m [kg]	I [kg·m^2]	m [kg]	I [kg·m^2]	m [kg]	I [kg·m^2]							
00	41.8	0.255	158.0	0.654	8.2	0.0114	OLD	1:2	500	180	350	20	180
04	34.0	0.175	119.5	0.592	8.2	0.0114	OLD	1:2	500	180	350	20	180
07	34.0	0.175	119.5	0.592	8.2	0.0114	OLD	1:2	600	180	350	20	180
13	34.0	0.175	119.5	0.592	6.7	0.0053	NEW	1:2.5	600	180	350	20	180
15	34.0	0.175	119.5	0.592	6.7	0.0053	NEW	1:2.5	600	120	350	20	180

3. Results

From the simulations results were obtained, among others, courses of parameters of the driving torque and the main shaft angular velocity, see Fig. 5. When compared individual starts of the machine from the main shaft position 180°, the initial configuration 00 has the slowest start contrary to the 13, which

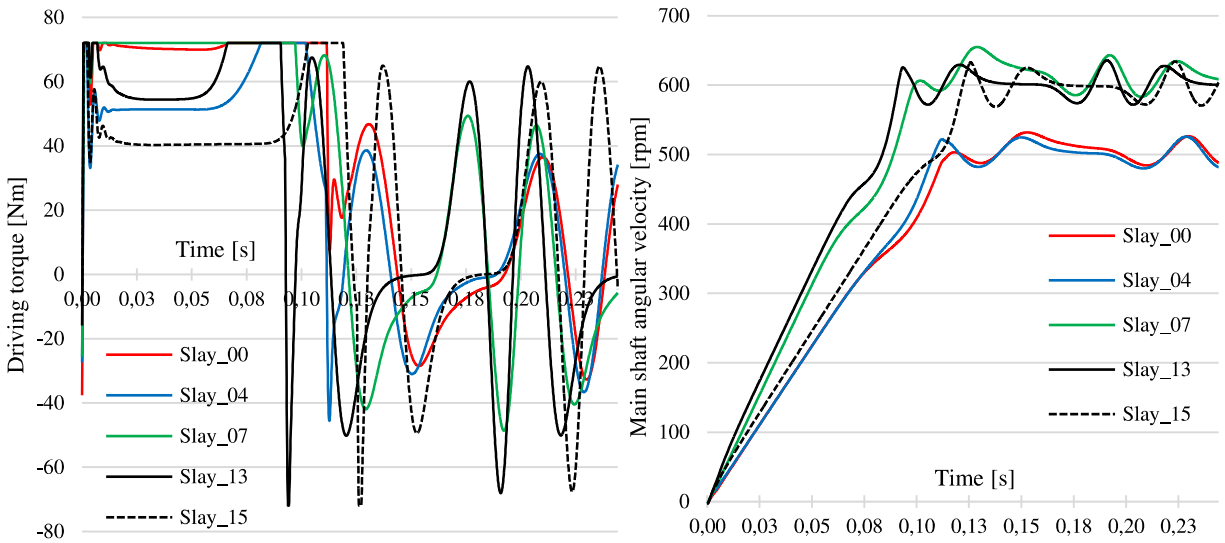

Fig. 5: Simulated drive torque and main shaft angular velocity during a start of the machine

reaches the nominal speed in the shortest time. Simulation 07 shows that the maximum driving torque of 72 Nm is required in a entire time interval 0 – 0.1 s. Mainly by the change of the belt gear ratio, simulation 13, compared to the 07, shows in the time interval 0.02 – 0.06 decreased torque of 54 Nm. When the start is from the main shaft position 120°, the required torque is in the time interval 0.02 – 0.09 further lowered to 40 Nm.

The higher weaving speed, the changed displacement law and the decreased moment of inertia, however, naturally result in raised driving torque requirements during a steady state in the range from -68 to 65 Nm for simulations 13 and 15 compared to the range from -31 to 37 Nm for the simulation 00 of the initial state. Despite that, it is still in the range of an available torque of the actual electric motor.

4. Conclusions

The simulations results show that the application of all the particular adjustments of the slay mechanism leads to improvements in terms of driving torque requirements during the start of the machine, even though, the increased weaving speed reaches 600 *rpm*.

The results obtained by the simulations were assessed prior to the production of modified components, including production and assembly jigs. The optimized slay mechanism will significantly help to fulfil the requirements for increased machine productivity and the quality of the final product. When the new slay mechanism is mounted on the machine, verifications of the simulations results will be included in a further complex measurement of the dynamical behaviour of the DIFA machine.

Acknowledgement

This work has been elaborated in the framework of project TM02000031 “The Production Technology Performance Increase and Distance Fabrics Utility Properties Extension for New Applications”.

References

Åström, J.K. and Murray, M.R. (2008) *Feedback Systems: An Introduction for Scientists and Engineers*. Princeton University Press, Princeton, NJ. ISBN 978-0-691-13576-2.

Bose, B.K. (2002) *Modern power electronics and AC drives.* Upper Saddle River: Prentice Hall PTR. ISBN 0-13-016743-6.

Koňařík T., Zbončák R. and Žák J. (2022) Optimization of the Batten of the Weaving Loom DIFA. In: Beran J., Bílek M., Václavík M. and Žabka P. (eds) *Advances in Mechanism Design III. TMM 2020. Mechanisms and Machine Science*, vol 85. Springer, Cham, doi: 10.1007/978-3-030-83594-1_35

Ondrášek J. and Karel P. (2020) The Model of a Controlled Mechanical System of an Air-Jet Loom Shedding Mechanism. In: Pisla D., Corves B., Vaida C. (eds) *New Trends in Mechanism and Machine Science. EuCoMeS 2020. Mechanisms and Machine Science*, vol 89. Springer, Cham, doi: 10.1007/978-3-030-55061-5_12